# Theoretical description of quantum beats of recoil-free $\gamma$ radiation

J. E. Monahan and G. J. Perlow
*Physics Division, Argonne National Laboratory, Argonne, Illinois 60439*
(Received 26 March 1979)

A classical optical theory is given for the phenomenon of $\gamma$-ray quantum beats observed by Perlow in a study of the Mössbauer effect of a frequency-modulated source. The intensity $I(\omega_0 - \omega_0', t)$ of the radiation from such a source transmitted through a resonant absorber is obtained as a function of $\omega_0 - \omega_0'$ and $t$, where $\omega_0'$ is the frequency of an absorber resonance, $\omega_0$ is the central frequency of the frequency-modulated source, and $t$ is the laboratory time. An average is taken over the unobserved initial formation time of the excited nuclear state in the source. When viewed at fixed $\omega_0 - \omega_0'$, the calculated intensity displays beats in the time spectrum, and when viewed at fixed $t$, the intensity shows dispersion at appropriate values of $\omega_0 - \omega_0'$, responsible for the observed enhancement of intensity above background. The harmonic content of the quantum beats is calculated explicitly in the thin-absorber limit, and the observed linear variation about $\omega_0 - \omega_0' = 0$ of the ratio of Fourier components $D_1/D_2$ is explained. The use of $D_1/D_2$ to measure small frequency shifts is analyzed by a statistical comparison with the method of switching between steepest points of the line, as used in gravitational-red-shift measurements. The variances are comparable. The effect on $I(\omega_0 - \omega_0', t)$ of line broadening due to sample inhomogeneities is calculated for a Lorentz distribution of center frequencies in source and absorber, and a prescription is given for modifying the various terms in $I(\omega_0 - \omega_0', t)$ accordingly. Finally, the effect of a distribution of phase and amplitude of the motion of the vibrating source is discussed.

## I. INTRODUCTION

Recently measurements have been reported[1] of the transmission of frequency-modulated recoil-free $\gamma$-rays through a resonant absorber. Interesting time- and frequency-dependent behavior of the transmitted radiation was observed. The present article contains a theoretical explanation of these results.

The experimental situation of Ref. 1 is illustrated in Fig. 1 and is described in detail in the caption. Briefly three sorts of measurement were made: (a) normal Mössbauer velocity spectra, (b) time spectra, in which the interval between a count and a reference time associated with the frequency modulation was obtained and accumulated, and (c) velocity spectra, in which the time measurement supplied a gate for excluding all but a portion of the events, such that the accepted ones lay in some chosen interval of the frequency modulation cycle. Figures 2–4 show examples. The captions are self-explanatory.

The experiments analyzed here are clearly related to the phenomenon of time filtering,[2–6] but there is one qualitative difference. The present experiments do not employ a previous nuclear event to determine the origin of time. Our counting rates are typically 500–1000/sec, two orders of magnitude higher than is practical in a coincidence experiment.

Consider a $\gamma$-ray source that is vibrated sinusoidally with angular frequency $\Omega$ and amplitude $x_0$ along the direction of observation. The time dependence of the field amplitude associated with this radiation can be written as

$$E(t, t_0) = \begin{cases} \lambda^{1/2} \exp[i\omega_0 t - \frac{1}{2}\lambda(t - t_0) + ia \sin\Omega t\,], & t \geq t_0 \\ 0, & t < t_0 \end{cases} \tag{1.1}$$

where $\lambda^{-1}$ is the mean lifetime of the decaying state, $\omega_0$ is the unperturbed frequency of the emitted radiation, and $a = \omega_0 x_0/c$ is called the modulation index. The decaying state is formed at time $t_0$ and the zero of the laboratory time $t$ is chosen as a zero of the sine in Eq. (1.1). Since $t_0$ is not measured, the observed intensity of this radiation is

$$\int_{-\infty}^{\infty} dt_0 |E(t, t_0)|^2 = 1, \tag{1.2}$$

and its frequency spectrum is

$$\int_{-\infty}^{\infty} dt_0 |E(\omega, t_0)|^2 = \sum_{n=-\infty}^{\infty} \frac{J_n^2(a)}{(\omega - \omega_0 - n\Omega)^2 + \frac{1}{4}\lambda^2} . \tag{1.3}$$

Here $J_n(a)$ is a Bessel function of the first kind and $E(\omega, t_0)$ is the Fourier transform of Eq. (1.1). [Note that, if $t_0$ were measured, the spectrum $|E(\omega, t_0)|^2$ would involve a double summation.]

Spectra of the form of Eq. (1.3) were first observed by Ruby and Bolef[7] with Mössbauer radia-

 

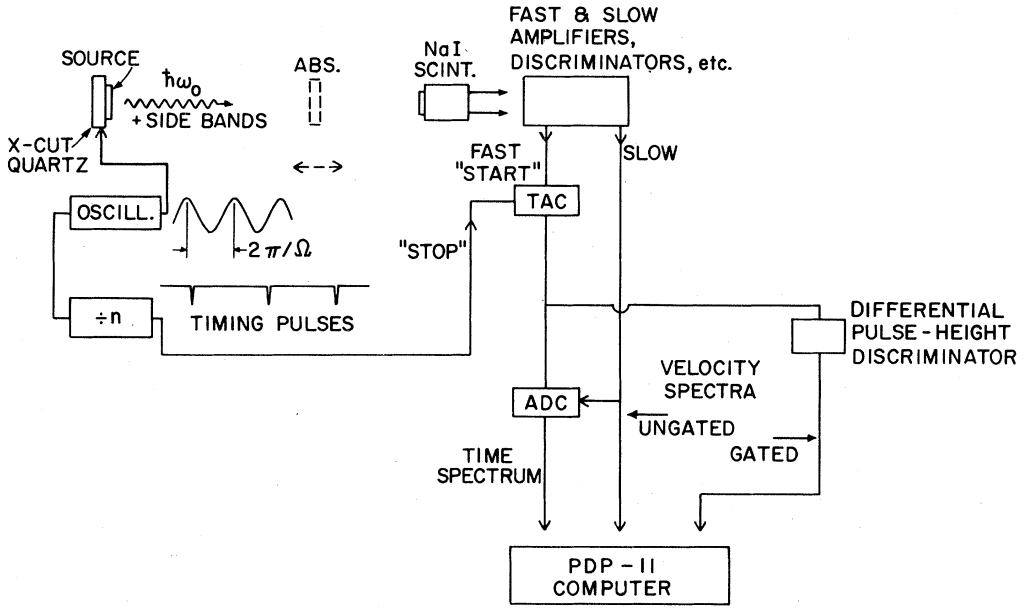


FIG. 1. Experimental conditions underlying the theory in this paper. An $x$-cut quartz piezo-crystal has cemented to one face a thin copper foil into which $^{57}$Co has been diffused. The 14.4-keV Mössbauer radiation exits the foil, passes through any of several selectable absorbers, and is detected at the right in a sodium iodide scintillation counter. The piezo-crystal vibrates at 9.95 MHz as a result of voltage applied to it from an oscillator. The latter is also counted down by some chosen multiple (typically 5 or 10) and provides timing pulses at a constant phase with respect to the crystal motion. From the scintillation counter one derives pulses for a slow and a fast channel. They are separately amplified in appropriate amplifiers and pass through appropriate differential discriminators to select the pulse heights. A time-to-amplitude converter (TAC) measures the interval between an acceptable event in the fast channel and the next occurring timing pulse. The TAC output consists of pulses whose heights depend linearly on these time intervals. It is recorded in the PDP-11 computer by means of an analog-to-digital converter (ADC). Alternatively, a velocity spectrum may be made in the normal manner, by moving an absorber (at a frequency of a few hertz) and storing the pulses from the slow channel in the computer operated as a time-mode analyzer. This gives a normal Mössbauer velocity spectrum. However, it is also possible by means of a differential discriminator, and the analog pulses from the TAC, to store similarly only those events that occur during a specified phase interval of the motion of the source. This produces a *time-gated* velocity spectrum.

tion and in various connections by many others since.[8-10] In practice, the relative intensities of the various sidebands usually are not correctly described by Eq. (1.3), a point which Abragam[11] and others have discussed and to which we shall return in Sec. V.

In Sec. II we calculate the intensity $I(t,\Delta\omega)$ of the radiation described by Eq. (1.1) after it has been transmitted through an absorber containing a resonance whose frequency is $\omega_0'$. Here $t$ is the laboratory time and $\Delta\omega=\omega_0-\omega_0'$. The intensity $I(t,\Delta\omega)$ contains interference terms between different frequency components which account for the beats that are observed when, for fixed values of $\Delta\omega$, the intensity is measured as a function of $t$. As discussed in Sec. III, this beat phenomenon may be used for the precise measurement of small energy shifts. Dispersion effects observed in time-gated frequency spectra $\int_{t_1}^{t_2} dt\, I(t,\Delta\omega)$ are considered in Sec. IV.

The analysis presented in Secs. II–IV is based on the assumption of ideal motion of the source (with unique modulation index $a$) and on the further assumption that there is no line broadening other than that due to the absorber thickness. In Sec. V the analysis of the previous sections is modified to include nonuniform motion of the source and excess linewidths (attributable, for example, to a distribution of isomer shifts or to small quadrupole or magnetic splittings). The line broadening is treated in the approximation that the distribution of resonance frequencies is Lorentzian.

## II. THEORY

In this section the classical optical theory used by Lynch, Holland, and Hamermesh[3] to describe the transmission of recoil-free $\gamma$-rays through a resonant absorber is extended to include the vibrational motion of the source.

We first make use of the Jacobi-Anger formula

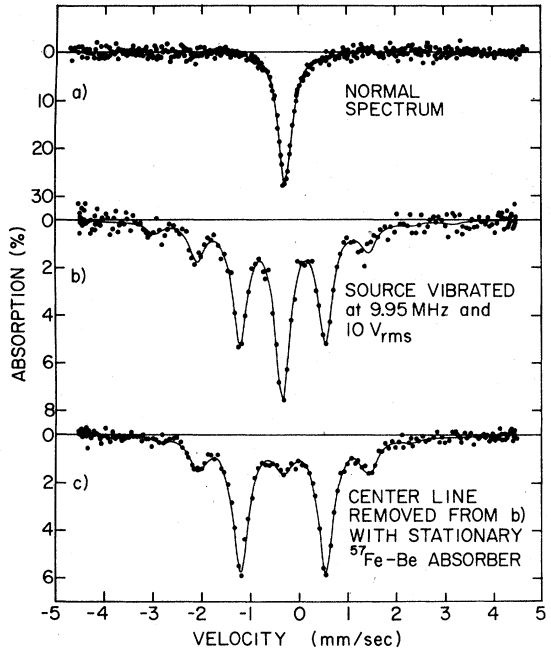


FIG. 2. (Reproduced from Ref. 1.) Three ungated velocity spectra. Figure 2(a) is the spectrum of the $^{57}$Co-Cu source recorded by moving an absorber of sodium ferrocyanide enriched in $^{57}$Fe. Figure 2(b) shows the frequency modulation one obtains by vibrating the source with a quartz piezo-crystal. Figure 2(c) shows a similar spectrum in which a stationary absorber of $^{57}$Fe-Be has been interposed between the source and the analyzing sodium ferrocyanide.

$$e^{ia\sin\Omega t} = \sum_{n=-\infty}^{\infty} J_n(a) e^{in\Omega t}$$

to rewrite Eq. (1.1) in the form

$$E(t, t_0) = \lambda^{1/2} \sum_{n=-\infty}^{\infty} J_n(a) e^{i\omega_n t_0} \frac{1}{2\pi i} \int_{-\infty}^{\infty} d\omega\, c_n(\omega) , \tag{2.1}$$

$$c_n(\omega) = e^{i\omega(t-t_0)}/(\omega - \omega_n - \tfrac{1}{2}i\lambda) , \tag{2.2}$$

where $\omega_n = \omega_0 + n\Omega$ is the frequency of the $n$th sideband. If this radiation passes through an absorber, each monochromatic component $c_n(\omega)$ is altered such that $c_n(\omega) \to c_n'(\omega)$, where

$$c_n'(\omega) = c_n(\omega) \exp[2ib\omega/(\omega^2 - \omega_0'^2 - i\omega\lambda)] . \tag{2.3}$$

The resonant frequency of the absorber, $\omega_0'$, may be varied by Doppler effect to obtain a frequency (velocity) spectrum.

The connection between angular frequency units and the usual velocity units of Mössbauer spectroscopy for the 14.413-keV radiation of $^{57}$Fe is: 7.305 $\times 10^7$ rad/sec = 1 mm/sec, $\omega_0 = 2.190 \times 10^{20}$ rad/sec. The natural linewidth of the excited nuclear state is $\lambda = 7.09 \times 10^6$ rad/sec = 0.0970 mm/sec and $2\lambda$ is the narrowest absorption linewidth observable by Mössbauer spectroscopy. The quantity $\Omega$ in the experiments was typically $6.252 \times 10^7$ rad/sec (corresponding to 9.95 MHz). In Eq. (2.3), $b$ is a constant that depends on the thickness of the absorber; at $\omega = \omega_0'$, Eq. (2.3) becomes

$$c_n'(\omega_0') = c_n(\omega_0') \exp(-2b/\lambda) ,$$

so that the transmission of a monochromatic radiation at the center of the resonance is $\exp(-4b/\lambda)$. In terms of conventional Mössbauer parameters $b/\lambda = \frac{1}{4} n \sigma_0 f_a$, where $n$ is the number of resonant nuclei/cm$^2$, $\sigma_0$ the peak cross section, and $f_a$ the recoil-free fraction of the absorber.

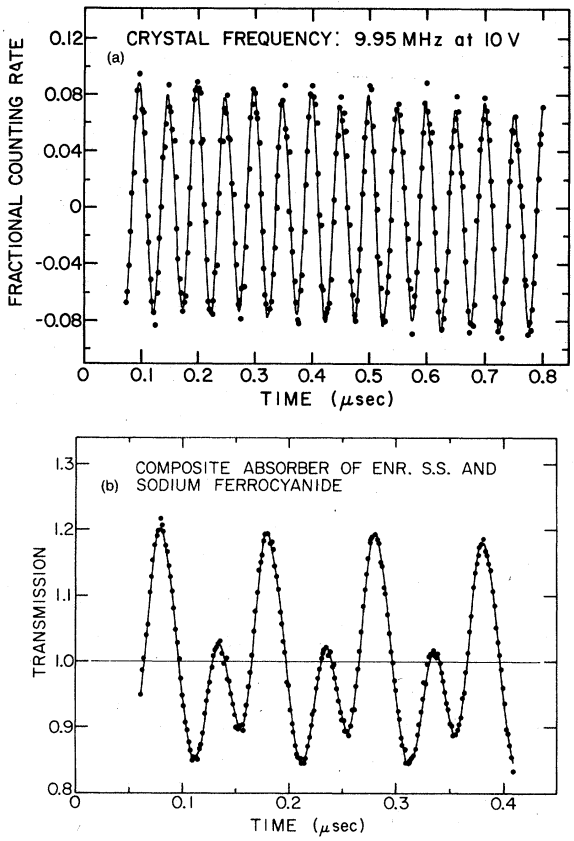


FIG. 3. Quantum beats. (a) With vibrating source and stationary $^{57}$Fe-Be absorber, the time spectrum contains principally the second harmonic of the modulation frequency ($2\Omega = 19.90$ MHz $\times 2\pi$). Figure 3(b) is made by replacing the Fe-Be with a composite absorber of stainless steel and sodium ferrocyanide. It has an isomer shift of $-0.3$ mm/sec with respect to the source. The fundamental (i.e., the modulation) frequency now dominates.

Consider next the integral in Eq. (2.1) with $c_n(\omega)$

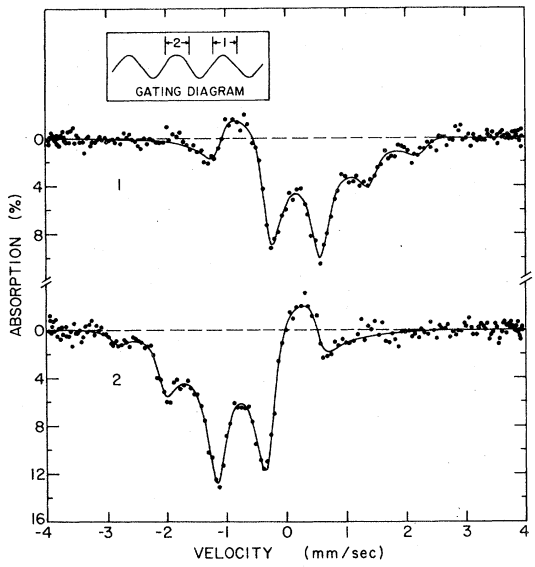


FIG. 4. Time-gated velocity spectrum. In order to set the gating intervals, a $^{57}$Fe-Be absorber is temporarily installed and the beat spectrum of Fig. 3(a) is obtained. As shown in Fig. 1, a differential pulse-height discriminator can then be used to select events during the desired phase interval. The selection is diagrammed at the top of the figure. Two cycles of the beat correspond to one cycle of crystal motion. The gate having been set, the $^{57}$Fe-Be absorber is removed, the sodium ferrocyanide analyzing absorber is installed, and a gated velocity spectrum is made. With respect to the crystal motion, the two gates have widths $\Omega\Delta t = \pi/2$ and are separated by $\pi$.

replaced by $c_n'(\omega)$, Eq. (2.3). The contribution to this integral from the singularity at $\omega = -(\omega_0'^2 - \frac{1}{4}\lambda^2)^{1/2} + \frac{1}{2}i\lambda$ is proportional to $b/\omega_0'$ and can be neglected since $b \ll \omega_0'$. Furthermore, since $\lambda \ll \omega_0'$, we have to a good approximation

$$2ib\omega(\omega^2 - \omega_0'^2 - i\omega\lambda)^{-1} = ib(\omega - \omega_0' - \tfrac{1}{2}i\lambda)^{-1} . \quad (2.4)$$

It follows that the amplitude $E(t, t_0)$ of the transmitted radiation is

$$E'(t, t_0) = \lambda^{1/2} \sum_{n=-\infty}^{\infty} J_n(a) e^{i\omega_n t_0} \frac{1}{2\pi i} \int_{-\infty}^{\infty} d\omega\, c_n'(\omega) , \quad (2.5)$$

$$c_n'(\omega) = \exp[\, i\omega(t - t_0)\,] (\omega - \omega_n - \tfrac{1}{2}i\lambda)^{-1} \times \exp[ib(\omega - \omega_0' - \tfrac{1}{2}i\lambda)^{-1}] . \quad (2.6)$$

The time and frequency dependence of the intensity of the transmitted radiation is obtained by integration of $|E'(t, t_0)|^2$ over the unobserved time $t_0$:

$$I(t, \Delta\omega) = \lim_{T\to\infty} \int_{-T}^{t} dt_0 |E'(t, t_0)|^2 . \quad (2.7)$$

Considered as functions of $t_0$, the frequency integration as well as the sum over $n$ in Eq. (2.5) converge uniformly in the interval $-T \leq t_0 < t$ and we assume that this is sufficient to justify the commutation of the various operations implied in Eq. (2.7). Equation (2.7) can then be rewritten in the form

$$I(t, \Delta\omega) = (2\pi)^{-2}\lambda \sum_{n=-\infty}^{\infty} \sum_{l=-\infty}^{\infty} J_n(a) J_l(a) e^{i(\omega_n - \omega_l)t} \times \lim_{T\to\infty} \int_{-\infty}^{\infty} d\omega \int_{-\infty}^{\infty} d\omega'\, f_n(\omega) f_l^*(\omega') \times F_{nl}(\omega, \omega') , \quad (2.8)$$

where

$$f_n(\omega) = (\omega - \omega_n - \tfrac{1}{2}i\lambda)^{-1} \exp[ib(\omega - \omega_0' - \tfrac{1}{2}i\lambda)^{-1}], \quad (2.9)$$

$$F_{nl}(\omega, \omega') = \frac{1 - e^{-i(\omega' - \omega + \omega_n - \omega_l)(T+t)}}{i(\omega' - \omega + \omega_n - \omega_l)} . \quad (2.10)$$

For fixed values of $\omega'$, $F_{nl}(\omega, \omega')$ has no singularities in the complex $\omega$ plane and as $\mathrm{Im}\,\omega \to \infty$, $F_{nl}(\omega, \omega') \to 0$. Similarly, for fixed values of $\omega$, $F_{nl}(\omega, \omega')$ has no singularities in the complex $\omega'$ plane and as $\mathrm{Im}\,\omega' \to -\infty$, $F_{nl}(\omega, \omega') \to 0$.

This is a particularly convenient result since the only contributions to the frequency integrals in Eq. (2.8) are from the singularities of the functions $f_n(\omega)$ and $f_l^*(\omega')$. Thus, for example, the integral over $\omega$ in Eq. (2.8) is evaluated as

$$\int_{-\infty}^{\infty} d\omega f_n(\omega) F_{nl}(\omega, \omega') = 2\pi i \oint_{\omega_n + i\lambda/2} d\omega f_n(\omega) F_{nl}(\omega, \omega') + 2\pi i \oint_{\omega_0' + i\lambda/2} d\omega f_n(\omega) F_{nl}(\omega, \omega') , \quad (2.11)$$

where the contour $(-\infty, \infty)$ has been closed by a semicircle in the upper half of the $\omega$ plane. The remaining integral over $\omega'$ is similarly evaluated by closing the contour $(-\infty, \infty)$ my means of a semicircle in the lower half of the $\omega'$ plane. The result is

$$I(t, \Delta\omega) = 1 + \sum_{n=-\infty}^{\infty} \sum_{l=-\infty}^{\infty} J_n(a) J_l(a) G_{nl}(\Delta\omega) \times \exp[i(n - l)\Omega t] , \quad (2.12)$$

where

$$G_{nl}(\Delta\omega) = -1 + \exp\{ib[(\Delta\omega + n\Omega)^{-1} - (\Delta\omega + l\Omega + i\lambda)^{-1}]\}$$
$$+ \sum_{k=1}^{\infty} \frac{(ib)^k}{k!(k-1)!} \frac{d^{k-1}}{dz^{k-1}} \left[\left(\frac{1}{z - \Delta\omega - n\Omega} - \frac{1}{z - \Delta\omega - n\Omega + i\lambda}\right)\exp\left(\frac{-ib}{z + (l-n)\Omega + i\lambda}\right)\right]_{z=0} . \quad (2.13)$$

Since $G_{nl}(\Delta\omega)$ is, by construction, Hermitian, i.e.,

$$G_{nl}(\Delta\omega) = G^*_{ln}(\Delta\omega) , \quad (2.14)$$

the apparent singularity at $\Delta\omega + n\Omega = 0$ must cancel in Eq. (2.13) to all orders of $b/\lambda$. With $G_{nl}$ written as a sum of terms arranged in increasing powers of $b$,

$$G_{nl}(\Delta\omega) = \sum_{m=1}^{\infty} G^{(m)}_{nl}(\Delta\omega) , \quad (2.15)$$

relations (2.13) and (2.14) can be used to show that

$$G^{(1)}_{nl}(\Delta\omega) = ib\left(\frac{1}{N - i\lambda} - \frac{1}{L + i\lambda}\right), \quad G^{(2)}_{nl}(\Delta\omega) = \frac{b^2}{L - N + i\lambda}\left(\frac{1}{N - i\lambda} - \frac{1}{L + i\lambda}\right) - \frac{b^2}{2}\left(\frac{1}{(N - i\lambda)^2} + \frac{1}{(L + i\lambda)^2}\right),$$
$$\cdots \quad (2.16)$$
$$G^{(m)}_{nl}(\Delta\omega) = (-ib)^m \sum_{\kappa=1}^{m} \frac{1}{\kappa!(m-\kappa)!} \frac{1}{(L - N + i\lambda)^{m-\kappa}}\left(\frac{1}{(L + i\lambda)^{\kappa}} + \frac{(-)^{\kappa}}{(N - i\lambda)^{\kappa}}\right)$$
$$+ (-ib)^m \sum_{\kappa=2}^{m-1} \frac{1}{\kappa!(m-\kappa)!} \sum_{s=1}^{\kappa-1} \binom{m+s-\kappa-1}{s} \frac{1}{(L - N + i\lambda)^{m+s-\kappa}}\left(\frac{1}{(L + i\lambda)^{\kappa-s}} + \frac{(-)^{\kappa-s}}{(N - i\lambda)^{\kappa-s}}\right),$$

where $L = \Delta\omega + l\Omega$, $N = \Delta\omega + n\Omega$, and $\binom{x}{y}$ is the binomial coefficient.

An indication of the rate of convergence of the expansion (2.15) can be obtained as follows. From Eqs. (2.16) it is clear that convergence is slowest for $L = N = 0$, i.e., for $l = n$ and $\Delta\omega = -n\Omega$. In this case, Eqs. (2.16) reduce to

$$G^{(m)}_{nn}(\Delta\omega = -n\Omega) = (-b/\lambda)^m \frac{(2m)!}{(m!)^3} . \quad (2.17)$$

For any given value of $b/\lambda$ there exists an integer $M$ such that for all values of $m \geq M$,

$$|G^{(m+1)}_{nn}(\Delta\omega = -n\Omega)| < |G^{(m)}_{nn}(\Delta\omega = -n\Omega)| . \quad (2.18)$$

Since Eq. (2.15) is an alternating series, it follows that the error incurred by truncation of the sum (2.15) at $m = m' \geq M$ is less than

$$(b/\lambda)^{m'+1} \frac{(2m'+2)!}{[(m'+1)!]^3} .$$

Thus, for $b/\lambda = \frac{1}{4}$, truncation at $m' = 3$ would result in an error of less than $\pm 0.012$ (or $< 3.6\%$) for any of the coefficients $G_{nl}(\Delta\omega)$ at any value of $\Delta\omega$. For $b/\lambda = 1$, truncation at $m' = 10$ gives an error less than $\pm 0.017$ (or $< 2.6\%$).

Equation (2.12) with the $G_{nl}$ given by Eq. (2.16) can be examined for a limiting case. If we set the modulation index $a$ to zero, the transmitted intensity is no longer time dependent and Eq. (2.12) reduces to

$$I(t, \Delta\omega) = I(\Delta\omega) = 1 + G^{(1)}_{00}(\Delta\omega) + G^{(2)}_{00}(\Delta\omega) + \cdots$$
$$= 1 - \frac{2b\lambda}{(\Delta\omega)^2 + \lambda^2} + \frac{2b^2\lambda^2}{[(\Delta\omega)^2 + \lambda^2]^2}$$
$$+ \frac{b^2}{(\Delta\omega)^2 + \lambda^2} + \cdots . \quad (2.19)$$

If the absorber is thin this can be approximated by

$$I(\Delta\omega) \approx \exp\left(-\{2b\lambda/[\Delta\omega^2 + \tfrac{1}{4}(2\lambda)^2]\}\right), \quad (2.20)$$

which describes a line that is thickness broadened in excess of the minimum width $2\lambda$. Its transmission at resonance is $e^{-2b/\lambda}$, the exponent being half that for a monochromatic radiation at the line center.

Equations (2.12) and (2.16) contain time-dependent absorption and dispersion terms. Let us rewrite (2.12) in the form

$$I(t, \Delta\omega) = I_1 + I_2 + I_3 , \quad (2.21)$$

where

$$I_1 = 1 + J_0^2(a)G_{00}(\Delta\omega) + 2\sum_{n=1}^{\infty} J_n^2(a)G_{nn}(\Delta\omega) ,$$

$$I_2 = \sum_{n=-\infty}^{\infty} \sum_{\substack{l=-\infty \\ (l\neq n)}}^{\infty} J_n(a)J_l(a)\cos[(n-l)\Omega t]\,\mathrm{Re}\{G_{nl}\} ,$$

$$I_3 = -\sum_{n=-\infty}^{\infty} \sum_{\substack{l=-\infty \\ (l\neq n)}}^{\infty} J_n(a)J_l(a)\sin[(n-l)\Omega t]\,\mathrm{Im}\{G_{nl}\} .$$

If data are taken without reference to time, one must average over $t$ in (2.21) and then $I_2 = I_3 = 0$. The remaining term $I_1(\Delta\omega)$ describes the time-independent frequency spectrum of the frequency-modulated source as observed by transmission through an absorber whose energy is varied.

In the thin-absorber approximation we have

$$\mathrm{Re}\{G_{nl}\} \approx \mathrm{Re}\{G_{nl}^{(1)}\} = -b\lambda\left(\frac{1}{N^2+\lambda^2} + \frac{1}{L^2+\lambda^2}\right)$$

$$\mathrm{Im}\{G_{nl}\} \approx \mathrm{Im}\{G_{nl}^{(1)}\} = b\left(\frac{N}{N^2+\lambda^2} - \frac{L}{L^2+\lambda^2}\right) , \qquad (2.22)$$

and, in particular

$$G_{nn}^{(1)} = -2b\lambda/(N^2+\lambda^2)$$

is real. To this approximation, each transmitted sideband in $I_1$ has the Lorentz shape with full width $2\lambda$ at half maximum, and absorption dip equal to $1 - 2b/\lambda$.

If the sidebands are well separated, i.e., if $\Omega \gg \lambda$, then because of the denominators in $\mathrm{Re}\{G_{nl}^{(1)}\}$ and $\mathrm{Im}\{G_{nl}^{(1)}\}$, $I_2$ and $I_3$ are small except if $\omega_0'$ is close to a sideband frequency $\omega_0 + n\Omega$, and then only one of the two terms in parentheses in Eqs. (2.22) is important. In these regions, $I_2$ is an even function of $\Delta\omega$ around $n\Omega$ and therefore describes a time-varying absorption (or its opposite, depending on the phase of the cosine). Contrarily, $I_3$ is an odd function of $\Delta\omega$ around $n\Omega$ and describes time-varying dispersion. This simplicity disappears in higher orders. An expression in real form to first and second order in $b/\lambda$ is given in the Appendix.

The normalization in Eq. (2.12) is such that with thickness parameter $b/\lambda = 0$ (i.e., with no absorber) $I(t,\Delta\omega) = 1$. However, when $b/\lambda > 0$, there are values $t'$, $\Delta\omega'$ for which $I(t',\Delta\omega') > 1$, corresponding to an *enhancement* of intensity. Thus, for specific values of $t$ and $\Delta\omega$ the insertion of an absorber actually increases the intensity of the transmitted beam. This can be attributed to a storage phenomenon in which the intensity at $t'$ is due to an accumulation over previous time. It is a temporal equivalent to spatial diffraction.

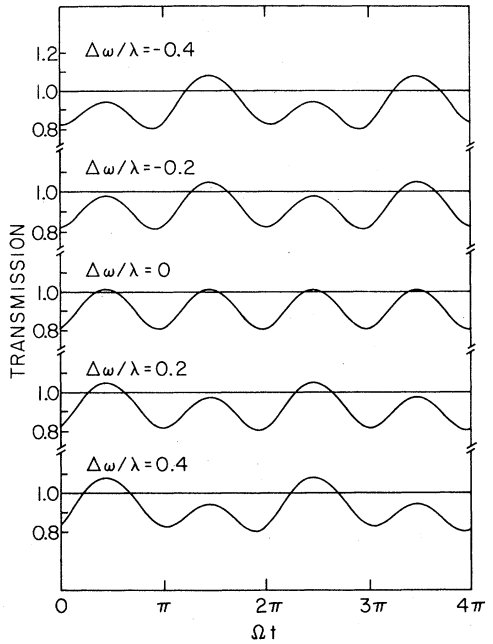


FIG. 5. Calculated quantum beats. The transmitted intensity $I(t,\Delta\omega)$ plotted at various fixed values of $\Delta\omega$ as a function of laboratory time. $I(t,\Delta\omega) = 1$ corresponds to the absence of absorber. The calculation is to second order in $b/\lambda$. The parameters used are $a = 1.5$, $b/\lambda = \frac{1}{4}$. The source and absorber are assumed to be $^{57}$Fe in unsplit form with natural linewidth, and the vibration frequency of the source is $\Omega/2\pi = 9.95$ MHz.

For fixed values of $\Delta\omega$, the transmitted intensity $I(t,\Delta\omega)$ exhibits beats that contain the frequency $\Omega$ and its harmonics. (See the experimental spectra in Fig. 3.) Passage through the resonant absorber changes a frequency-modulated photon into one with some amplitude modulation. The time dependence is due to interference between different frequency components of the photon amplitude. It is an individual quantum phenomenon and by analogy with the usage in optics has been called *quantum beats*.

In Fig. 5 we display a series of calculated time spectra characterized by various fixed values of $\Delta\omega/\lambda$. The magnitude of the quantities used are those given in the text following Eq. (2.3) with $a = 1.5$ and $b/\lambda = \frac{1}{4}$. The calculations are to second order in $b/\lambda$. At $\Delta\omega/\lambda = 0$, the spectrum contains only even harmonics, of which the second dominates. The odd harmonics emerge as $|\Delta\omega|$ increases.

Figure 6 displays a series of spectra in which $\Delta\omega$ is varied with various fixed values of $t$. What is actually plotted is an average of $I(t,\omega)$ over a

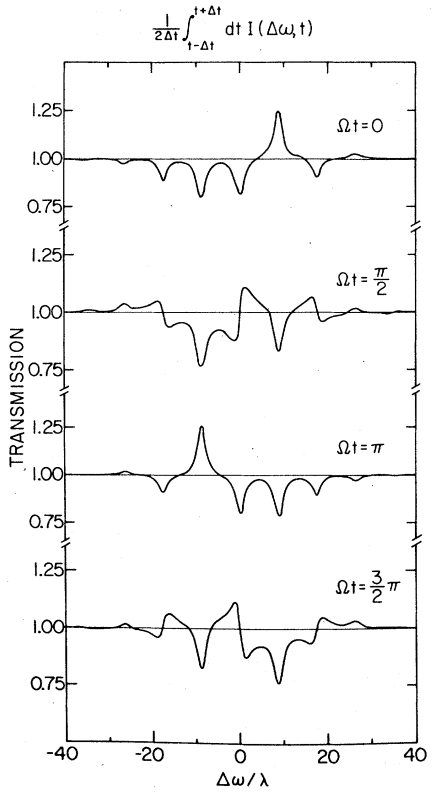


FIG. 6. $\bar{I}(t,\omega)$ as a function of $\omega$ for various fixed values of $t$. The transmission $\bar{I}(t,\omega)$ is an average over a small region $\pm\Delta t$ about $t$. The calculation is to second order with the same parameters as in Fig. 5.

small time interval about $t$. The dispersion is readily apparent. The constants are as in Fig. 5.

The complexity of the entire $I(t,\Delta\omega)$ surface may be seen in the three-dimensional plot of Fig. 7. We show only the region from $\Omega t = 0$ to $\Omega t = \pi$. The region from $\pi$ to $2\pi$ replicates it with mirror symmetry.

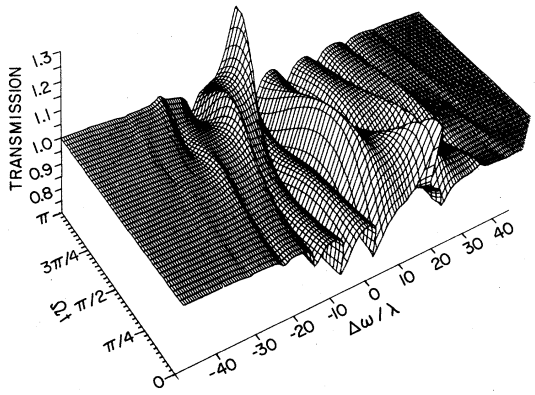


FIG. 7. Surface $I(t,\Delta\omega)$ plotted against both variables. The region from $\Omega t = \pi$ to $\Omega t = 2\pi$ (not shown) may be obtained by reflection in the plane perpendicular to the $\Omega t$ axis at $\Omega t = \pi$. The parameters are those of Fig. 5.

## III. HARMONIC CONTENT OF QUANTUM BEATS

In this section we consider the analysis of the phenomenon exhibited in Fig. 8. As pointed out in Ref. 1 it is potentially useful for sensitive experiments, e.g., the measurement of relativistic energy shifts.[12] This potential exists because the harmonic composition of the beat spectrum $I(t,\Delta\omega)$ is sensitive to small changes in the value of $\Delta\omega$ in the neighborhood of $\Delta\omega = 0$. To see this consider its Fourier series representation,

$$I(t,\Delta\omega) = \sum_{j=0}^{\infty} D_j(\Delta\omega)\cos[j\Omega(t-\tau_j)]. \tag{3.1}$$

From Eq. (2.12) it follows that

$$D_0(\Delta\omega) = 1 + \sum_{l=-\infty}^{\infty} J_l^2(a) G_{ll}(\Delta\omega)\ , \tag{3.2}$$

$$D_j(\Delta\omega)e^{ij\Omega\tau_j} = 2\sum_{l=-\infty}^{\infty} J_l(a)J_{l-j}(a)G_{l-jl}(\Delta\omega), \quad j>0\ . \tag{3.3}$$

To first order in $b/\lambda$, we have from Eqs. (2.16)

$$G_{ll}^{(1)}(\Delta\omega) = \frac{-2b\lambda}{(\Delta\omega + l\Omega)^2 + \lambda^2}\ , \tag{3.4}$$

$$G_{l-jl}^{(1)}(\Delta\omega) = -b\lambda\left(\frac{1}{(\Delta\omega + l\Omega)^2+\lambda^2} + \frac{1}{[\Delta\omega + (l-j)\Omega]^2+\lambda^2}\right) + ib\left(\frac{\Delta\omega + (l-j)\Omega}{[\Delta\omega + (l-j)\Omega]^2+\lambda^2} - \frac{\Delta\omega + l\Omega}{(\Delta\omega + l\Omega)^2+\lambda^2}\right), \tag{3.5}$$

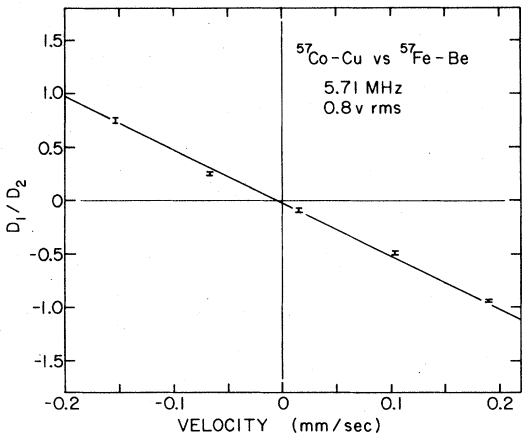


FIG. 8. Ratio D1/D2. Fourier analysis of time spectra, such as those in Fig. 3, leads to this plot of the ratio D1/D2 of the fundamental to second-harmonic amplitude as a function of shift. The data were obtained by using a moving Fe-Be absorber but utilizing only a small interval of velocity for each data point. The data were taken at 5.71 MHz.

In the case of interest, $\Delta\omega < \lambda < \Omega$, the main contributions to the sum in Eq. (3.3) are those for which $l=0$ and $l=j$, and only terms with resonance denominator $(\Delta\omega)^2+\lambda^2$ in Eq. (3.5) need to be retained. Equation (3.3) can thus be written approximately as ($j>0$)

$$D_j(\Delta\omega)e^{ij\Omega\tau_j} = \frac{2bJ_0(a)J_j(a)}{(\Delta\omega)^2+\lambda^2} \times\{-\lambda[1+(-1)^j]+i\Delta\omega[1-(-1)^j]\}. \tag{3.6}$$

For even values of $j$ the right-hand side of Eq. (3.6) is real, and hence

$$\sin j\Omega\tau_j = 0 ,$$

$$D_j(\Delta\omega) = -4b\lambda J_0(a)J_j(a)/[(\Delta\omega)^2+\lambda^2], \tag{3.7}$$

and $|D_j(\Delta\omega)|$ has a maximum at $\Delta\omega=0$. For odd values of $j$,

$$\cos j\Omega\tau_j = 0 ,$$

$$D_j(\Delta\omega) = 4bJ_0(a)J_j(a)\Delta\omega/[(\Delta\omega)^2+\lambda^2], \tag{3.8}$$

which has extrema at $\Delta\omega=\pm\lambda$. Thus for $j$ odd, we have

$$\frac{D_j(\Delta\omega)}{D_{j+1}(\Delta\omega)} = -\frac{J_0(a)J_j(a)}{J_0(a)J_{j+1}(a)}\frac{\Delta\omega}{\lambda} . \tag{3.9}$$

Note that, for small values of $\Delta\omega$, the ratio $D_1/D_2$ of the fundamental to the second harmonic of the oscillator frequency is a linear function of the frequency difference $\Delta\omega$ and is zero when $\Delta\omega=0$. Even without the approximations introduced in the derivation of Eq. (3.9), numerical calculations show that the linearity is excellent over most of the interval $-1\leq\Delta\omega/\lambda\leq 1$.

Some measure of the sensitivity of the method described above can be obtained by comparing it with previous measurements of small frequency shifts. In particular, let us consider the measurement of the gravitational red shift carried out by Pound and collaborators[13] and by Cranshaw and Schiffer.[14] These experiments were done in transmission geometry with source and detector at the top and bottom of a tower. To measure the small gravitational shift, a velocity-switching scheme was employed that shifted the source $\gamma$-ray energy back and forth between the steepest parts of the absorption curve of the resonant absorber. The gravitational shift is deduced from the difference in the two counting rates. It is easily shown that the standard deviation $\sigma_{\Delta\omega}$ (due only to counting statistics) in the value of the frequency shift $\Delta\omega$ determined in this manner is

$$|\sigma_{\Delta\omega}| = \frac{4}{3\sqrt{3}}\frac{\Gamma}{\alpha\sqrt{N_t}} , \tag{3.10}$$

where $\Gamma$ is the experimental width of the absorption line, $N_t$ is the total number of counts recorded in the measurement, and $\alpha$ is the fractional absorption; $0<\alpha\leq 1$.

In order to get the corresponding quantity $\sigma'_{\Delta\omega}$ for a measurement by the method of quantum beats, we assume for convenience that the data are divided into $n$ equally spaced time intervals covering one cycle ($2\pi/\Omega$) of the fundamental frequency. The data $I(t_k,\Delta\omega)$ are to be fitted to the Fourier series equation (3.1) by the method of least squares; i.e., one is to find the amplitudes $D_j$ and the time phases $\tau_j$ that minimize the quantity $Q$, where

$$Q = \frac{n}{N_t}\sum_{k=1}^{n}\left(I(t_k,\Delta\omega) - \frac{N_t}{n}\sum_{j=0}^{\infty}D_j\cos j\Omega(t_k-\tau_j)\right)^2 . \tag{3.11}$$

Suppose the modulation index $a$ is chosen such that terms in the sum over $j$ in Eq. (3.11) are unimportant for $j>2$ and that the variance of $D_2$ is negligible. This will generally be true for $\Delta\omega \ll \lambda$, in which case $D_1 \ll D_2$. From the theory of least squares we obtain for the variance of $D_1$

$$\sigma_{D_1}^2 = \frac{2}{\partial^2 Q/\partial^2 D_1} = \frac{2}{2\frac{N_t}{n}\sum_{k=1}^{n}\sin^2\frac{2\pi k}{n}} = \frac{2}{N_t} . \tag{3.12}$$

By use of Eq. (3.9) it follows that

$$|\sigma'_{\Delta\omega}| = \frac{\lambda}{|D^2|}\left|\frac{J_2(a)}{J_1(a)}\right|\left(\frac{2}{N_t}\right)^{1/2} \tag{3.13}$$

and for the ratio of the quantum-beat method to the velocity-switching method we have

$$\left|\frac{\sigma'_{\Delta\omega}}{\sigma_{\Delta\omega}}\right| = \left(\frac{3}{2}\right)^{3/2}\frac{\alpha}{|D_2|}\left|\frac{J_2(a)}{J_1(a)}\right|\frac{\lambda}{\Gamma} = \frac{3\sqrt{3}}{4\sqrt{2}}\frac{\alpha}{2b/\lambda}\frac{\lambda}{\Gamma}\frac{1}{|J_0(a)J_1(a)|} , \tag{3.14}$$

where Eq. (3.7), with $\Delta\omega^2 \ll \lambda^2$, has been used to eliminate $D_2$ from the right-hand side of this equation. In the thin-absorber approximation, $\alpha/(2b/\lambda)\cong 1$, $\lambda/\Gamma\cong\frac{1}{2}$, and Eq. (3.14) reduces to

$$|\sigma'_{\Delta\omega}/\sigma_{\Delta\omega}| \cong [\,8\sqrt{2}\,/3\sqrt{3}\,|J_0(a)J_1(a)|\,]^{-1} . \tag{3.15}$$

The product $|J_0(a)J_1(a)|$ has a maximum value of $\sim 0.34$ at $a=1.08$, so that

$$|\sigma'_{\Delta\omega}/\sigma_{\Delta\omega}| \geq 1.4 . \tag{3.16}$$

The inequality in Eq. (3.16) is introduced in anticipation of modification discussed in Sec. V. If all parts of the source do not vibrate with the same amplitude and phase the factor, then $|J_0(a)J_1(a)|$ in Eq. (3.15) must be replaced by an average $|\langle J_0(a)J_1(a)e^{i\chi}\rangle|$ over the appropriate distribution of the modulation index $a$ and the phase angle $\chi$, a subject considered more fully in Sec. V. In general this averaging will increase the value of the ratio $|\sigma'_{\Delta\omega}/\sigma_{\Delta\omega}|$. For the success of the present method it is important that the source be prepared such that these effects are minimized.

## IV. TIME-GATED FREQUENCY SPECTRA

It is possible to set a time gate over an interval of the beat spectrum by use of a differential pulse-height discriminator set on the output pulses of a time-to-amplitude converter. (See Fig. 1.) With pulses counted only during the interval $t_1 \leq t \leq t_2$, the measured frequency spectrum will be

$$\frac{1}{t_2-t_1}\int_{t_1}^{t_2} dt\, I(t,\Delta\omega)=\frac{1}{\theta_2-\theta_1}\int_{\theta_1}^{\theta_2} d\theta I(\theta/\Omega,\Delta\omega)$$

$$=1+\sum_{l=-\infty}^{\infty}\sum_{\substack{n=-\infty\\(n\neq l)}}^{\infty} J_l(a)J_n(a)G_{nl}(\Delta\omega)\frac{e^{i(n-l)\theta_2}-e^{i(n-l)\theta_1}}{i(n-l)(\theta_2-\theta_1)}+\sum_{l=-\infty}^{\infty}J_l^2(a)G_{ll}(\Delta\omega), \quad (4.1)$$

where $\theta=\Omega t$. In this section some of the properties of these spectra are discussed.

Figure 4 shows two such experimental gated spectra in which the gating intervals were of length $\pi$ on successive maxima of second-harmonic beats. This corresponds to $\theta_2-\theta_1=\pi/2$ for each spectrum with the lower limits $\theta_1$ differing by $\pi$ for the two runs. The spectra are mirror images about $v=-0.28$ mm/sec, which is the relative isomer shift of the $^{57}$Co-Cu source and the sodium ferrocyanide absorber and corresponds to $\Delta\omega=0$. The mirror symmetry, namely

$$\int_{\theta_1}^{\theta_2} d\theta I(\theta/\Omega,\Delta\omega)=\int_{\theta_1+\pi}^{\theta_2+\pi} d\theta I(\theta/\Omega,-\Delta\omega)\,, \quad (4.2)$$

is a consequence of the relations

$$G_{nl}(-\Delta\omega)=G_{-l-n}(\Delta\omega)\,, \quad (4.3)$$

which follow from the definitions (2.16).

By an appropriate choice of the gating interval all or part of the interference that gives rise to the beat phenomenon may be eliminated. The choice $\theta_2-\theta_1=2\pi$ clearly corresponds to an average overall time and hence to no gating at all. Inspection of (4.1) shows that there will be no contribution from the interference of the $l$th and $n$th sidebands if $\theta_2-\theta_1$ is chosen such that $\exp[i(n-l)(\theta_2-\theta_1)]=1$.

In Fig. 9, we display a set of theoretical spectra with the time interval increasing from $\theta_2-\theta_1\approx 0$ to $\theta_2-\theta_1=2\pi$. When $\theta_2-\theta_1=2\pi$ one sees the normal time-independent frequency-modulation spectrum. As the limits of integration shrink toward zero, the dispersion peaks appear, until the spectrum becomes identical with one of those shown in Fig. 7.

## V. MODIFICATIONS OF THEORY

The analysis described in Sec. II–IV is based on the assumptions that the motion of the source can be described in terms of a unique value of the modulation index and that the natural linewidths for emission and absorption are observable. Normally these assumptions cannot be fully justified. The perturbations caused by lines broadened owing to inhomogeneity and by nonuniformities in the motion of the source are discussed in this section.

The line-broadening problem is considered in the approximation that the distributions of resonance-center frequencies (for emission and absorption) are Lorentzian. Thus, for example, the equation

$$L(\omega_0)d\omega_0=\frac{\gamma_s}{2\pi}\frac{d\omega_0}{(\omega_0-\eta_s)^2+\frac{1}{4}\gamma_s^2} \quad (5.1)$$

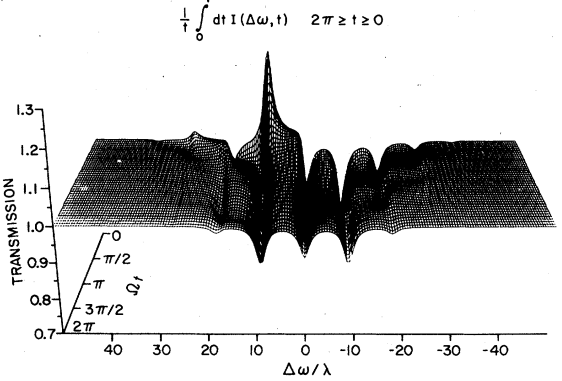


FIG. 9. Transition from the time-independent frequency spectrum (foreground) to the spectrum with dispersion, depending on the size of the averaging interval. The parameters are those of Fig. 5.

describes the distribution for emission. The distribution for absorption $L'(\omega_0')d\omega_0'$ is similarly defined with $\gamma_s$ and $\eta_s$ in Eq. (5.1) replaced by $\gamma_a$ and $\eta_a$. The transmitted intensity then is

$$I = \int_{-\infty}^{\infty} d\omega_0 \int_{-\infty}^{\infty} d\omega_0' L(\omega_0)L'(\omega_0')I(t,\Delta\omega)$$

$$= 1 + \sum_{n=-\infty}^{\infty} \sum_{l=-\infty}^{\infty} e^{i(n-l)\Omega t} J_n(a)J_l(a)$$

$$\times \int_{-\infty}^{\infty} \int d\omega_0\, d\omega_0' L(\omega_0)L'(\omega_0')G_{nl}(\Delta\omega) , \quad (5.2)$$

where $\Delta\omega = \omega_0 - \omega_0'$. It is obvious that it is intensity rather than amplitude that should be averaged over the source distribution. It can also be shown that, for this case, an intensity average over the absorber distribution is also correct.

Consider first the integration over $\omega_0'$. The $G_{nl}$, considered as functions of $\omega_0'$, are defined in Eqs. (2.15) and (2.16) as sums of terms of the form $(\omega_0' - \omega_0 - k\Omega \pm i\lambda)^n$ with poles either in the upper or lower half of the complex $\omega_0'$ plane. Since $n \geq 0$, we have

$$\int_{-\infty}^{\infty} \frac{d\omega_0' L'(\omega_0')}{(\omega_0' - \omega_k \pm i\lambda)^n} = \frac{1}{[\eta_a - \omega_k \pm i(\lambda + \frac{1}{2}\gamma_a]^n} , \quad (5.3)$$

where $\omega_k = \omega_0 + k\Omega$. The right-hand side of Eq. (5.3), considered as a function of $\omega_0$, has poles in the upper or lower half of the complex $\omega_0$ plane so that an identical argument applies to the integration over $\omega_0$. If we now identify $\eta_a - \eta_b$ as $\Delta\omega$, the final result of the integration, Eq. (5.2), is to replace $\Delta\omega \pm i\lambda$ in the $G_{nl}(\Delta\omega)$ with $\Delta\omega \pm i\lambda'$, where

$$\lambda' = \lambda + \tfrac{1}{2}(\gamma_a + \gamma_s) . \quad (5.4)$$

With this change Eqs. (2.16) become

$$G_{nl}^{(m)}(\Delta\omega) = (-ib)^m \sum_{\kappa=1}^{m} \frac{1}{\kappa!(m-\kappa)!} \frac{1}{L - N + i\lambda)^{m-\kappa}} \left( \frac{1}{(L + i\lambda')^{\kappa}} + \frac{(-)^{\kappa}}{(N - i\lambda')^{\kappa}} \right)$$

$$+ (-ib)^m \sum_{\kappa=2}^{m-1} \frac{1}{\kappa!(m-\kappa)!} \sum_{s=1}^{\kappa-1} \binom{m+s-\kappa-1}{s} \frac{1}{(L - N + i\lambda)^{m+s-\kappa}} \left( \frac{1}{(L + i\lambda')^{\kappa-s}} + \frac{(-)^{\kappa-s}}{(N - i\lambda')^{\kappa-s}} \right) , \quad (2.16')$$

where, for $m = 1$ and 2, the second sum over $\kappa$ vanishes and, as before, $L \equiv \Delta\omega + l\Omega$, $N \equiv \Delta\omega + n\Omega$. Note that both $\lambda$ and $\lambda'$ appear in these equations. However, the lowest-order terms $G_{nl}^{(1)}(\Delta\omega)$ contains only $\lambda'$, so that the results derived (to lowest order) in Sec. III can be restated by the simple replacement $\lambda \to \lambda'$. This applies to Eqs. (3.4)–(3.8) and (3.14).

Next we consider the modification of the formalism that is necessary to take into account the fact that there is generally a distribution in both phase and amplitude (but not frequency) of motion over the source dimensions. Since a photon originates at a single nucleus in the source, it is the *intensity* that must be averaged over this distribution.

The effect of adding a phase $\chi$ to the argument of the sine in Eq. (1.1) is to multiply the $n$, $l$ term of the double sum in Eq. (2.12) by the factor $\exp[i(n-l)\chi]$. The transmitted intensity of radiation from such a source is then

$$I(t,\Delta\omega) = 1 + \sum_{n=-\infty}^{\infty} \sum_{l=-\infty}^{\infty} \langle J_n(a)J_l(a)e^{i(n-l)\chi}\rangle \times G_{nl}(\Delta\omega)e^{i(n-l)\Omega t} , \quad (5.5)$$

The brackets $\langle \cdots \rangle$ denote an average of $\cdots$ over the joint distribution of the modulation index $a$ and the phase angle $\chi$. In general this distribution will depend on the method of preparation of the source.

If $a$ and $\chi$ are statistically independent and if $\chi$ is distributed normally about $\chi = 0$ with variance $\sigma^2$, then

$$\langle J_n(a)J_l(a)e^{i(n-l)\chi}\rangle = \langle J_n(a)J_l(a)\rangle \exp\{-\tfrac{1}{2}[(n-l)\sigma]^2\} , \quad (5.6)$$

and Eqs. (3.3) for the coefficients in the Fourier series representation of $I(t,\Delta\omega)$ become

$$D_j(\Delta\omega)e^{ij\Omega\tau_j} = 2e^{-(j\sigma)^2/2} \sum_{l=-\infty}^{\infty} \langle J_l(a)J_{l-j}(a)\rangle G_{l-jl}(\Delta\omega) . \quad (5.7)$$

Since the attenuation factor $\exp[-\frac{1}{2}(j\sigma)^2]$ is real, the effect of this distribution of phase is to replace the Fourier coefficient by $D_j'(\Delta\omega) = \exp[-\frac{1}{2}(j\sigma)^2]D_j(\Delta\omega)$. The attenuation rapidly becomes more severe with increasing values of $j$ and, in practice, sets a

limit to the highest statistically significant harmonic of the quantum beats.

If $\chi$ is independent of $a$ and randomly distributed over the interval 0 to $2\pi$, all Fourier coefficients except $D_0(\Delta\omega)$ vanish and no quantum beats will be seen. This is true for the distribution given by Abragam,[11] which has been shown by Cranshaw and Reivari[8] to be appropriate for a vibrating absorber with thickness greater than the ultrasonic wavelength. It has recently become possible, however, to obtain sources for which the $J_n^2(a)$ distribution is rather well displayed.[15]

ACKNOWLEDGMENT

This research was performed under the auspices of the Division of Basic Energy Sciences of the Department of Energy.

## APPENDIX

Equation (2.12) can be rewritten in a form that shows explicitly the absorptive and dispersive amplitudes of a given line. Let the intensity be written as a sum of terms arranged in increasing powers of the thickness parameter $b/\lambda$:

$$I(t,\Delta\omega)=1+\sum_{m=1}^{\infty} I^{(m)}(t,\Delta\omega)\ , \tag{A1}$$

where

$$I^{(m)}(t,\Delta\omega) = \sum_{n=-\infty}^{\infty}\sum_{l=-\infty}^{\infty} J_n(a)J_l(a) \times[\mathrm{Re}\{G_{nl}^{(m)}\}\cos\theta_{nl} - \mathrm{Im}\{G_{nl}^{(m)}\} \times \sin\theta_{nl}], \tag{A2}$$

$$\theta_{nl}=(n-l)\Omega t, \tag{A3}$$

and the $G_{nl}^{(m)}$ are defined by Eqs. (2.16). Equation (A2) can be written in the form

$$I^{(m)}(t,\Delta\omega)=-2b^m\sum_{n=-\infty}^{\infty}\frac{J_n(a)}{(\Delta\omega+n\Omega)^2+\lambda^2} \times[\lambda A_n^{(m)}-(\Delta\omega+n\Omega)B_n^{(m)}]. \tag{A4}$$

The thin-absorber case corresponds to retaining only the term with $m=1$ and displays the main interesting features of the spectrum. Here

$$A_n^{(1)}=J_0(a)\cos n\Omega t + \sum_{l=1}^{\infty} J_l(a)[\cos\theta_{nl}+(-)^l\cos\chi_{nl}], \tag{A5}$$

$$B_n^{(1)}=J_0(a)\sin n\Omega t + \sum_{l=1}^{\infty} J_l(a)[\sin\theta_{nl}+(-)^l\sin\chi_{nl}], \tag{A6}$$

$$\chi_{nl}=(n+l)\Omega t\ . \tag{A7}$$

The $n$th line contains the time-dependent absorption amplitude $2b\lambda J_n(a)A_n^{(1)}(t)$ and the dispersion amplitude $2bJ_n(a)B_n^{(1)}(t)$. The time dependence consists of harmonics of the fundamental angular frequency $\Omega$.

The term in $(b/\lambda)^2$ is obtained from

$$A_n^{(2)}=-\sum_{l=-\infty}^{\infty}\frac{J_l(a)}{(l-n)^2\Omega^2+\lambda^2}\left(\frac{\lambda^2-(l-n)^2\Omega^2}{2\lambda}\cos\theta_{nl}-(l-n)\Omega\sin\theta_{nl}\right)-\sum_{l=-\infty}^{\infty}\frac{J_l(a)}{(\Delta\omega+n\Omega)^2+\lambda^2}\lambda\cos\theta_{nl}, \tag{A8}$$

$$B_n^{(2)}\sum_{l=-\infty}^{\infty}\frac{J_l(a)}{(l-n)^2\Omega^2+\lambda^2}[(l-n)\Omega\cos\theta_{nl}+\lambda\sin\theta_{nl}]-\sum_{l=-\infty}^{\infty}\frac{J_l(a)}{(\Delta\omega+n\Omega)^2+\lambda^2}\lambda\sin\theta_{nl}\ . \tag{A9}$$

The terms in $A_n^{(m)}$ and $B_n^{(m)}$ with $m\geq 2$ that depend on $\Delta\omega$ give rise to thickness broadening.

[1]G. J. Perlow, Phys. Rev. Lett. 40, 896 (1978).
[2]R. E. Holland, F. J. Lynch, S. S. Hanna, and G. J. Perlow, Phys. Rev. Lett. 4, 181 (1960).
[3]F. J. Lynch, R. E. Holland, and M. Hamermesh, Phys. Rev. 120, 513 (1960).
[4]C. S. Wu, Y. K. Lee, N. Benczer-Koller, and P. Simms, Phys. Rev. Lett. 5, 432 (1960).
[5]S. M. Harris, Phys. Rev. 124, 1178 (1961).
[6]Applications of the altered line structure in time filtering have been made (among others) by K. Albrecht, U. Hauser, and W. Neuwirth, *Hyperfine Structure and Nuclear Radiations* (North-Holland, Amsterdam, 1968), p. 357; D. W. Hamill and G. R. Hoy, Phys. Rev. Lett. 21, 724 (1968); W. Triftshaüser and P. P. Craig, Phys. Rev. 162, 274 (1967).
[7]S. L. Ruby and D. I. Bolef, Phys. Rev. Lett. 5, 5 (1960).

[8]T. E. Cranshaw and P. Reivari, Proc. Phys. Soc. London 90, 1059 (1967).
[9]L. Pfeiffer, N. D. Heiman, and J. C. Walker, Phys. Rev. B 6, 74 (1972).
[10]G. J. Perlow, W. Potzel, R. M. Kash, and H. de Waard, J. Phys. (Paris) 35, C6-197 (1974).
[11]A. Abragam, *L'Effet Mössbauer* (Gordon and Breach, New York, 1964), pp. 22–24.
[12]See, for example, R. V. Pound, in *Workshop on New Directions in Mössbauer Spectroscopy*, edited by G. J. Perlow, AIP Conf. Proc. 38, 41 (1977), and references therein.
[13]R. V. Pound and G. A. Rebka, Jr., Phys. Rev. Lett. 4, 337 (1960); R. V. Pound and J. L. Snider, Phys. Rev. B 140, 788 (1965).
[14]T. E. Cranshaw and J. P. Schiffer, Proc. Phys. Soc. London 84, 245 (1964).
[15]L. E. Campbell and G. J. Perlow to be published.